Photostop of iodine atoms from electrically oriented ICl molecules*

Bao Da-Xiao(暴大小), Deng Lian-Zhong(邓联忠)†, Xu Liang(许 亮), and Yin Jian-Ping(印建平)

State Key Laboratory of Precision Spectroscopy, East China Normal University, Shanghai 200062, *China*

(Received 7 May 2015; published online 10 October 2015)

The dynamics of photostopping iodine atoms from electrically oriented ICl molecules was numerically studied based on their orientational probability distribution functions. Velocity distributions of the iodine atoms and their production rates were investigated for orienting electrical fields of various intensities. For the ICl precursor beams with an initial rotational temperature of ~ 1 K, the production of the iodine atoms near zero speed will be improved by about ~ 5 times when an orienting electrical field of ~ 200 kV/cm is present. A production rate of $\sim 0.5‰$ is obtained for photostopped iodine atoms with speeds less than 10 m/s, which are suitable for magnetic trapping. The electrical orientation of ICl precursors and magnetic trapping of photostopped iodine atoms *in situ* can be conveniently realized with a pair of charged ring magnets. With the maximal value of the trapping field being ~ 0.28 T, the largest trapping speed is ~ 7.0 m/s for the iodine atom.

Keywords: cold atoms, photodissociation, molecular orientation, magnetic trapping

PACS: 37.10.De, 87.15.mK, 37.90.+j, 37.10.Gh **DOI:** 10.1088/1674-1056/24/11/113702

1. Introduction

A number of methods and techniques have been developed for the generation of cold or ultracold atoms and molecules over the past decades. The technique of laser cooling and trapping has achieved great success in the production of ultracold atoms.[1,2] Ultracold molecules from the photoassociation of laser cooled atoms have also been reported.[3,4] Other methods, like buffer gas cooling,[5] low velocity filtering,[6] and deceleration with time-varying electric,[7] magnetic,[8] or optical[9] fields were also demonstrated in the production of cold molecules of chemical stability at room temperatures. Each method has its own advantages and disadvantages, and efforts in pursuit of new methods for cold atoms and molecules have never stopped. In recent years, a method called "Photostop", based on the photodissociation of precursor molecules, was demonstrated in the production of cold atoms[10] and molecules[11,12] near zero speed. Compared to other methods, Photostop features its minimal requirement on the experimental setup and its generality in the production of cold atoms and molecules.

The method of Photostop can prepare cold atoms and molecules inside a potential well and the decelerated particles near zero speed can be trapped *in situ*. Compared to other methods, there is no need for any loading process, which is usually inefficient. Rennick *et al.*[13] just demonstrated magnetic trapping of photostopped Br atoms with a pair of bar magnets. However, due to the finite angular distribution of the photofragmentation, the production rate of the decelerated particles trappable is relatively low. Recent theoretical study of our group has shown that the production rate of the decelerated Br atoms near zero speed can be greatly improved by working with laser aligned precursor Br_2 molecules.[14] When dipolar precursor molecules are used, the production of decelerated particles near zero speed can be improved by simply applying an electrical field for precursor orientation other than a strongly focusing laser pulse of high energy. The practice of orienting dipolar precursor molecules with electrical fields saves the expenditure on the aligning laser, frees the worry of precursor ionization in the focusing spot, and offers a large volume of precursor molecules for Photostop, though the improvement on the production of decelerated particles might not be much higher.

In this paper, we theoretically study the dynamics of photostopping iodine atoms from electrically oriented ICl precursors. The orientation of the ICl precursors exposed to electrical fields is investigated by calculating their orientational probability distribution functions. The dynamical photofragmentation of electrically oriented ICl precursors is simulated using the Monte Carlo method. The velocity distributions of the iodine atoms produced and their corresponding production rates are analyzed for orienting electrical fields of various intensities. Electrical orientation of precursor molecules and magnetic trapping of photostopped atoms *in situ* can be conveniently realized by using a pair of charged ring magnets.

2. Photostop of iodine atoms from electrically oriented ICl

2.1. Overview

The photodissociation of ICl molecules has been studied by De Vries *et al.*[15] and later by Bazalgette *et al.*[16] with

*Project supported by the National Natural Science Foundation of China (Grant Nos. 11034002, 61205198, and 11274114) and the National Key Basic Research and Development Program of China (Grant No. 2011CB921602).

†Corresponding author. E-mail: lzdeng@phy.ecnu.edu.cn

© 2015 Chinese Physical Society and IOP Publishing Ltd

electrical orientation. When the ground state ICl molecules are excited using photons around ~ 488 nm, the transition is almost purely parallel ($B0^+$-$X0^+$, i.e., the transition dipole moment $\boldsymbol{\mu}$ is parallel to the I–Cl bond and $\Delta\Omega = 0$). The excited molecule can dissociate via two channels. The minor channel leads to two atoms of the ground state ($I^2P_{3/2}$, $Cl^2P_{3/2}$) with a branching ratio of $\sim 21\%$; the major channel leads to one atom of the ground state ($I^2P_{3/2}$) and another atom of the spin–orbit excited state ($Cl^2P_{1/2}$) with a branching ratio of $\sim 79\%$. For simplicity of discussion, we consider the major product channel and focus our attention on the ground state iodine atom for the moment.

The basic idea of photostopping an iodine atom from an ICl molecule can be simply depicted as follows: a precursor ICl molecule moves with a velocity of $v_{\rm ICl}$ in the lab frame. After photodissociation, the two atoms (I and Cl) recoil along the molecular axis (or bond) in opposite directions with velocities of $u_{\rm I}$ and $u_{\rm Cl}$ in the center of mass (COM) frame. If the recoil velocity $u_{\rm I}$ of the iodine atom just cancels its original velocity $v_{\rm ICl}$, it will be brought to a standstill in the lab frame. This is why the name of "Photostop" is given. A detailed Newton diagram of Photostop can be found in Refs. [10] and [14]. The recoil speed of the ground state iodine atom in the center of mass frame (COM) is calculated as

$$u_{\rm I}=\sqrt{2E_{\rm kin}^{\rm avl}\frac{m_{\rm Cl^2P_{1/2}}}{m_{\rm I^2P_{3/2}}m_{\rm ICl}}}, \tag{1}$$

and

$$E_{\rm kin}^{\rm avl}=E_{\rm kin}^{\rm Cl^2P_{1/2}}+E_{\rm kin}^{\rm I^2P_{3/2}}=h\nu+E_{\rm int}^{\rm ICl}-D_0^{\rm ICl}-E_{\rm int}^{\rm I^2P_{3/2}+Cl^2P_{1/2}}, \tag{2}$$

with $h\nu$ being the photon energy, $E_{\rm int}^{\rm ICl}$ and $D_0^{\rm ICl}$ being the internal and dissociation energy of ICl, and $E_{\rm int}$ the internal energy of the respective atom or molecule.

2.2. Orientation of precursor molecules in electrical fields

Upon rigid rotor approximation, the Hamiltonian for a linear molecule exposed to electrical fields is given by $H = BJ(J+1) + W_{\rm Stark}$, where B is the rotational constant of the molecule, J is the quantum number of the rotational angular momentum, and $W_{\rm Stark} = -\boldsymbol{\mu}\cdot\boldsymbol{E}$ is the interaction between the electrical field (E-field) $\boldsymbol{E}$ and the electric dipole $\boldsymbol{\mu}$ of the molecule. The rotational levels $|JM\rangle$ of the molecule are adiabatically transformed into new eigenstates $|\tilde{}JM\rangle$, so called pendular states,[17] which can be expressed as a linear combination of the field free states $|JM\rangle$. The orientation of linear molecules is conventionally characterized by their orientational probability distribution function (OPDF) which indicates the distribution of the molecular axis orientation with respect to a specified axis (usually the direction of the external field). The OPDFs for symmetric top molecules exposed to an external E-field have been given by Wu *et al.*[18] For the linear ICl molecule, treated as a special case of the symmetric tops, the field dependent OPDF, $P_{JM}(\cos\theta, E)$, can be readily revised as

$$\begin{aligned} &P_{JM}(\cos\theta, E)\\ &= \int_0^{2\pi} {\rm d}\varphi \int_0^{2\pi} {\rm d}\chi \Psi_{JM}^*(E)\Psi_{JM}(E)\\ &= \sum_{J',J'',M',M''} a_{J'M'}^{JM} a_{J''M''}^{JM} \frac{\sqrt{(2J'+1)(2J''+1)}}{2}(-1)^{-M}\\ &\quad\times \sum_{n=|J'-J''|}^{J'+J''} (2n+1)\begin{pmatrix} J' & J'' & n\\ 0 & 0 & 0\end{pmatrix}\\ &\quad\times \begin{pmatrix} J' & J'' & n\\ M & -M & 0\end{pmatrix} {\rm P}_n(\cos\theta), \end{aligned} \tag{3}$$

in which $\Psi_{JM}(E) = |\tilde{}JM\rangle = \sum_{JM} a_{JM}|JM\rangle$ represents the wave function of the pendular state of the linear molecules in the E-field, ${\rm P}_n(\cos\theta)$ is the n-th order Legendre polynomial and the two preceding elements before ${\rm P}_n(\cos\theta)$ are 3-j symbols.

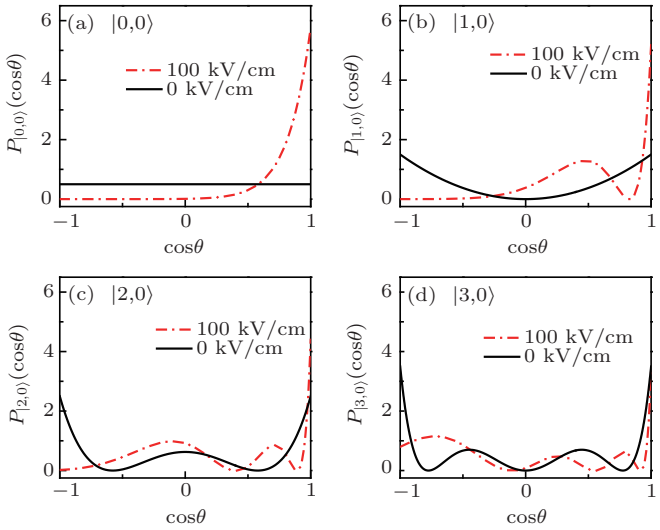


Fig. 1. (color online) Orientational probability distributions for ICl molecules of states (a) $|0,0\rangle$, (b) $|1,0\rangle$, (c) $|2,0\rangle$, (d) $|3,0\rangle$ with the electrical field strength being $E = 0$ kV/cm (solid line) and 100 kV/cm (dash dot line), respectively.

The degree of orientation of the dipole molecules depends on the magnitude of the external E-field. Figures 1(a)–1(d) show the orientational probability distribution (OPD) for ICl molecules ($B = 3422.39$ MHz, $\mu = 1.24$ Debye)[19] of states $|0,0\rangle$, $|1,0\rangle$, $|2,0\rangle$, and $|3,0\rangle$ being exposed to electrostatic fields of $E = 0$ kV/cm (solid line) and $E = 100$ kV/cm (dash dot line), respectively. Due to the dipole interaction with the external E-field, the ICl molecule has a larger probability oriented toward the direction of $\cos\theta = 1$, to which the electrical field $\boldsymbol{E}$ is pointed, as can be clearly seen from Figs. 1(a) and 1(b). Take the ICl molecules of state $|0,0\rangle$ for example, the orientational probability at $\cos\theta = 1$ will be increased by over ten-fold when the value of E rises up from 0 kV/cm

to 100 kV/cm. The OPDF of the dipolar molecule exposed to an orienting E-field has a strong dependence on its initial rotational energy. With the increasing rotational energy the molecule gets less tame to the external orienting E-field, as shown by the curves of OPDF in Figs. 1(a)–1(d) with increasing J value. For a molecule ensemble of rotational temperature T, the total OPD can be obtained by taking the average of the OPDs for all quantum states populated by the molecules with their respective thermal statistical weight, which is governed by the Boltzmann distribution law. Surely, the lower the molecule temperature T is, the more densely the lowest rotational states are populated, and thus the larger the degree of orientation of the molecule ensemble toward the external $\boldsymbol{E}$ field, as can be seen in Fig. 2.

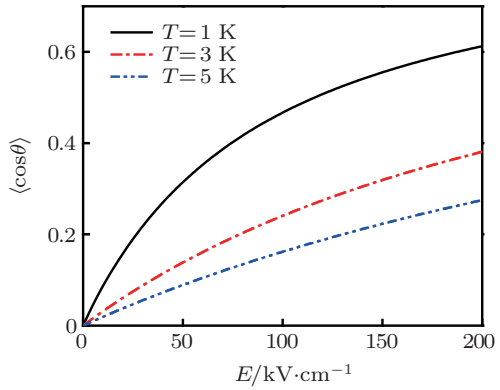


Fig. 2. (color online) Degree of orientation of the ICl molecule ensemble as a function of the external electric field with the ensemble temperature being 1 K (solid line), 3 K (dash dot line), and 5 K (dash dot dot line) respectively.

2.3. Dynamical simulation

For simplicity of discussion, $^{127}I^{35}Cl$ is used for simulations. The rotational temperature T of the ICl molecular beam is taken to be ~ 1 K with $J = 1$ being the most populated level. This temperature selection is based on the work of Kumarappan *et al.*,[20] who reported experimental study on the role of rotational temperature in adiabatic molecular alignment for a few molecular species with temperatures around ~ 1 K. The ICl molecular beam used for simulations has a mean velocity of ~ 301 m/s with a FWHM (full width at half maximum) spread of 30 m/s in the z (longitudinal) direction and a FWHM spread of 8 m/s centered at zero for each of the two transverse directions (x and y). The electrical field $\boldsymbol{E}$ for precursor orientation and the polarization of the laser field ($\lambda =\sim 488.0$ nm) for Photostop are both along the molecular beam axis (i.e., the z direction). The dissociation energy of the ground state ICl was chosen to be ~ 17365.80 cm^{-1} and the $^2P_{1/2} \rightarrow ^2P_{3/2}$ splitting is selected as ~ 882.35 cm^{-1}.[16] The dynamical fragmentation of ICl molecules exposed to orienting electrical fields of various intensities is simulated and the corresponding results are analyzed. Both product channels, as mentioned above, are considered during simulations.

Figures 3(a) and 3(b) show the velocity distributions of the ground state ($^2P_{3/2}$) iodine atoms after Photostop in the z direction and x or y direction, respectively. Results presented are for cases with the strength of the E-field for precursor orientation being 0 kV/cm (solid line), 50 kV/cm (dash dot dot line), 100 kV/cm (dash line), 150 kV/cm (dot line), and 200 kV/cm (dash dotline), respectively. Iodine atoms resulted from both product channels (the major channel ICl$\rightarrow$I$^2P_{3/2}$ + Cl$^2P_{1/2}$, and the minor channel ICl$\rightarrow$I$^2P_{3/2}$+Cl$^2P_{3/2}$) are discernible in the plot of Fig. 3(a) (solid line). The iodine atoms produced in the minor channel, who share more kinetic energy after Photostop, constitute the two outer small peaks (or shoulders exactly) adjacent to the inner big ones; whist the iodine atoms produced in the major channel, who share the right expected kinetic energy, form the two inner peaks. As we can see in both Figs. 3(a) and 3(b), the height of the peak corresponding to iodine atoms of zero velocity is increasing as the orienting E-field gets strong. This shows clearly the influence of the orienting E-field on improving the number of photostopped iodine atoms near zero speed.

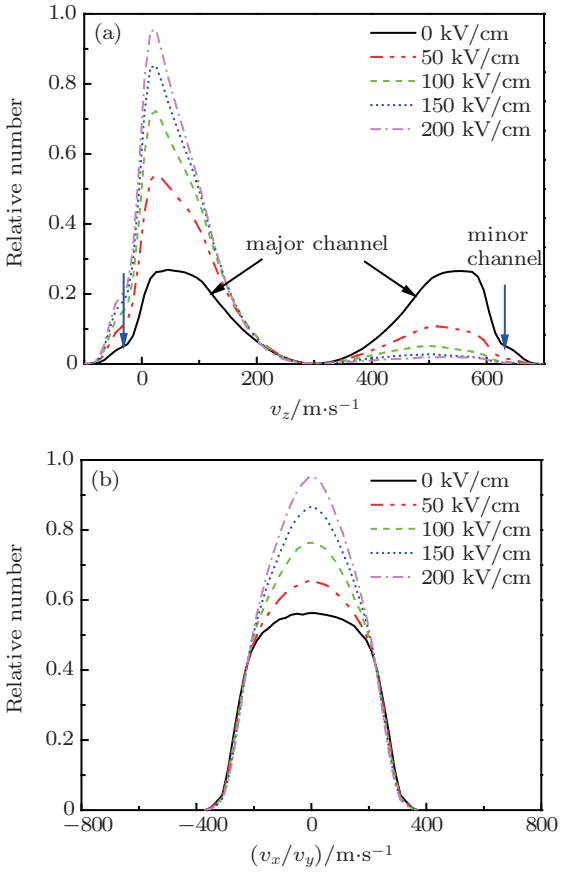


Fig. 3. (color online) The velocity distributions of the ground state ($^2P_{3/2}$) iodine atoms after photostop in the z direction (a) and x or y direction (b). The initial temperature T of the ICl precursor beam is ~ 1 K. The strength of the E-field for precursor orientation for each case is marked correspondingly on the upper right of the plot.

A more direct vision of the influence of the orienting E-field on the production of the ground state ($^2P_{3/2}$) iodine atoms

can be obtained by examining the total speed distribution, as shown in Fig. 4. Similarly, the results presented are for cases with the strength of the orienting E-field being 0 kV/cm (solid line), 50 kV/cm (dash dot dot line), 100 kV/cm (dash line), 150 kV/cm (dot line), and 200 kV/cm (dash dot line), respectively. There are two peaks for each curve in Fig. 4. The left peak corresponds mainly to the decelerated iodine atoms with the right one mainly to the accelerated iodine atoms. The area under the curve of each peak is proportional to the number of the corresponding iodine atoms. Without field, each iodine (or chlorine) atom has respective probabilities of 50% to recoil forward and backward during fragmentation in the COM. Thus the number of the decelerated atoms equals that of the accelerated ones, as shown by the equal area under the curve of the two peaks (solid line). With the increase of the orienting E-field strength, the left peak gets much higher with its apex moving closer to zero speed and the right peak gets much lower. The increasing area ratio of the left peak to the right one indicates that more iodine atoms are decelerated than accelerated as the orienting E-field gets stronger.

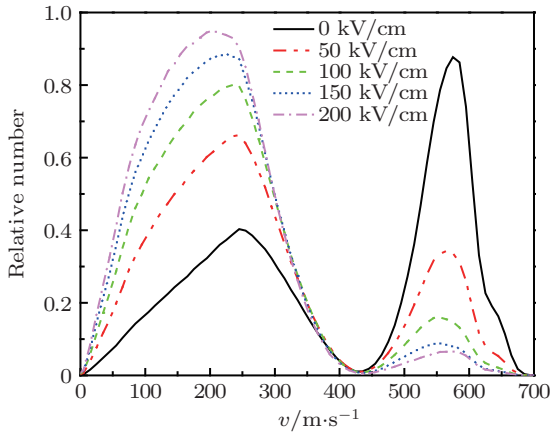


Fig. 4. (color online) The total speed distribution of the ground state iodine atoms after photostop. The initial temperature T of the precursor ICl molecules is ~ 1 K. The strength of the E-field for precursor orientation for each case is marked correspondingly on the plot.

The decelerated atoms with their speeds below a certain value (called truncated speed) are statistically counted. This count of the number of atoms starts from zero speed and proceeds toward high speeds with an interval of ~ 10 m/s. The impact of the orienting E-field on improving the production of the decelerated iodine atoms can be well understood by comparing the corresponding atom number to that of the case without E-field (i.e., $E = 0$ kV/cm). The corresponding ratio (also called the improvement factor) is plotted as a function of the truncated speed and shown in Fig. 5(a). Obviously, the largest improvement is obtained on photostopped atoms near zero speed. This is desirable since atoms of low speeds are of more interest. For instance, the improvement factors for the decelerated atoms of with speeds up to ~ 30 m/s are about ~ 1.0, ~ 2.5, ~ 3.5, ~ 4.5, and ~ 5.0 for cases with the orienting E-field intensity being 0 kV/cm (solid squares), 50 kV/cm (open circles), 100 kV/cm (open triangles), 150 kV/cm (open diamonds), and 200 kV/cm (open stars), respectively. With the increase of the truncated speed, the improvement factor decreases gradually and approaches unity for the ideal case of 100% photolysis of precursors. The production rate of the iodine atoms, defined as their number to the initial number of the precursor molecules, is plotted as a function of the truncated speed as well and shown in Fig. 5(b). For instance, the production rate for photostopped atoms with speeds ≤ 10 m/s is $\sim 0.1‰$, $\sim 0.2‰$, $\sim 0.3‰$, $\sim 0.4‰$, $\sim 0.5‰$ for cases with E-field strength being 0 kV/cm, (solid squares), 50 kV/cm (open circles), 100 kV/cm (open triangles), 150 kV/cm (open diamonds), and 200 kV/cm (open stars), respectively. The production rate of the iodine atoms increases sharply in the low speed region before continuing its gradual growth in the relatively high speed region. The limit of unity will be reached as the truncated speed increases to cover the whole speed distribution of all atoms for the ideal case of 100% photolysis of precursors.

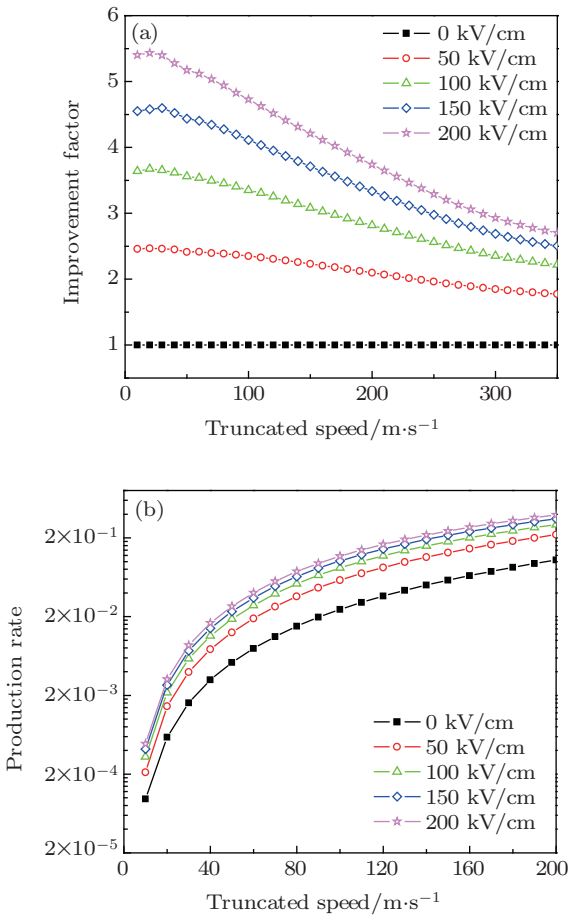


Fig. 5. (color online) The improvement factor (a) and the production rate (b) of the ground state iodine atoms ($^2P_{3/2}$) as a function of the truncated speed with E-field strength being 0 kV/cm (solid squares), 50 kV/cm (open circles), 100 kV/cm (open triangles), 150 kV/cm (open diamonds), and 200 kV/cm (open stars), respectively.

3. Prospects

Photostopped iodine atoms can be magnetically trapped for other researches. Magnetic trapping of atoms takes advantage of the Zeeman effect. The Hamiltonian of the Zeeman effect is $H_{\rm Zeeman} = -\mu_{\rm m} \cdot \boldsymbol{B}$, where $\mu_{\rm m}$ is the magnetic dipole moment of the atom and $\boldsymbol{B}$ is the magnetic field (B-field). With the electronic orbital and spin coupling (i.e., the fine structure) effect considered only, the potential of the atom due to the Zeeman effect can be simplified as $W_{\rm Zeeman} = g_J \mu_{\rm b} B J_{\rm m}$, where g_J is the Lande g factor and given by $g_J = 1 + [J(J+1) + S(S+1) - L(L+1)]/[2J(J+1)]$, with $\mu_{\rm b}$ being the Bohr magneton, and $J_{\rm m}$ the projection of J on the magnetic field. The above symbols S, L, and J are the quantum numbers for the electronic spin, orbital, and total angular momentum of the atom. The gradient force experienced by an atom in an inhomogeneous B-field is given by $F = -\nabla W_{\rm Zeeman} = -g_J \mu_{\rm b} J_{\rm m} \nabla B$. Therefore, atoms in states of positive $J_{\rm m}$, so called weak-field-seekers, will be repelled to the weak field region and those in states of negative $J_{\rm m}$, so called strong-field-seekers, will be attracted to the strong field region.

In 2014, Rennick *et al.*[13] reported the first experimental demonstration of trapping photostopped Br atoms with a pair of bar magnets. Here, we propose trapping photostopped iodine atoms from electrically oriented ICl molecules, as discussed above, with a pair of charged ring magnets. Figure 6 shows the schematic diagram of the proposal. A pulsed ICl molecular beam is traversing through the bores of the two ring magnets along direction z and being intercepted by a laser pulse propagating along direction x. The laser pulse for Photostop is polarized in the z direction (i.e., in parallel to the molecular beam axis). The outer diameter of the ring magnets is denoted as $D_{\rm o}$ with their inner diameter as $D_{\rm i}$. The thickness of the ring magnets is T with their face-to-face distance being L.

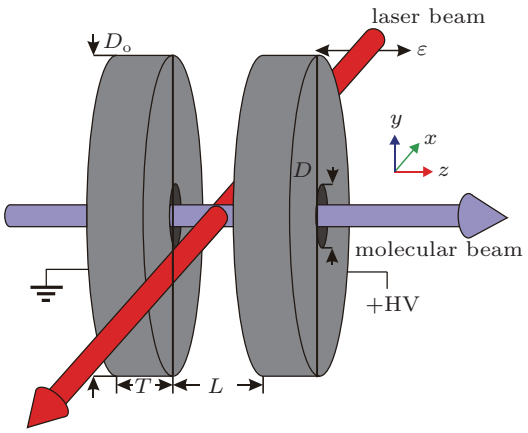


Fig. 6. (color online) Schematic diagram for magnetically trapping photostopped iodine atoms from electrically oriented ICl molecules.

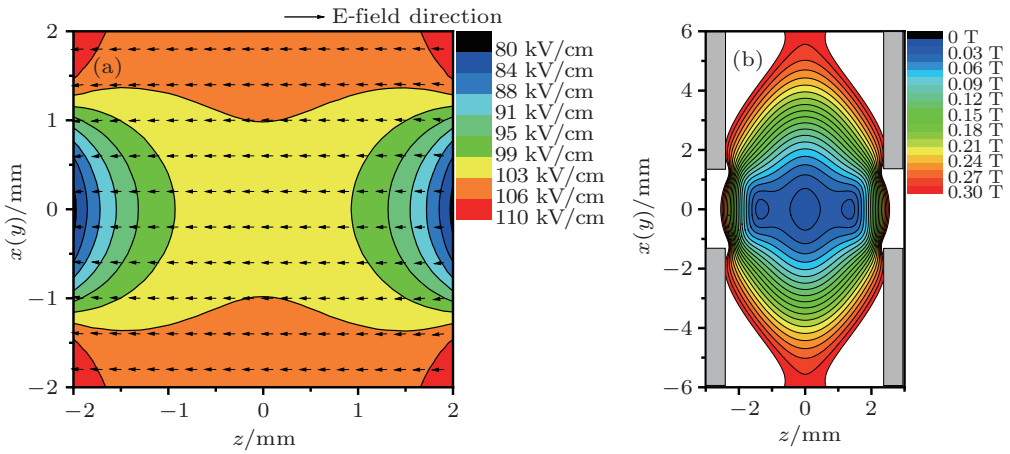


Fig. 7. (color online) E-field distribution between the charged ring magnets with geometric parameters being $D_{\rm o} = 12$ mm, $D_{\rm i} = 2.5$ mm, $T = 6$ mm, and $L = 5$ mm, respectively. The right ring magnet is connected to a high voltage of HV $= +53$ kV with its left counterpart at ground potential. (a) Contour plot in plane *xoz* (or *yoz*), the arrows pointing from right to left show the E-field directions; (b) contour plot of the magnetic field distribution generated by the pair of ring magnets with eminent magnetization $B_{\rm r} = 1.40$ T.

Figure 7 shows the contour plot of E-field distribution between the charged ring magnet and the contour plot of the B-field distribution generated by the pair of ring magnets with remnant magnetization $B_{\rm r} = 1.40$ T (available with commercial NdFeB permanent magnets from a number of producers, as can be found in http://www.hisupplier.com/a-ndfeb-magnet/). The arrows pointing from right to left in Fig. 7(a) show the E-field directions. The E-field keeps almost constant in the central area with a peak magnitude of ~ 100 kV/cm when HV $= +53$ kV. In Fig. 7(b) there exists a potential well with three centers of minimal B-field in the z direction. For the ground state iodine atoms ($^2{\rm P}_{3/2}$, $S = 1/2$, $L = 1$, $J = 3/2$, and $g_{\rm J} = 4/3$) $J_{\rm m}$ can take values of $-3/2$, $-1/2$, 1/2, and 3/2. This magnetic trap will be able to confine photostopped $I(^2{\rm P}_{3/2})$ atoms in the low field seeking $J_{\rm m} = 1/2$ and 3/2 states. The maximal value of the B-field forming the potential well is

about ~ 0.28 T, corresponding to maximal trapping speeds of ~ 4.0 m/s and ~ 7.0 m/s for iodine atoms of states $J_m = 1/2$ and 3/2, respectively. The total percentage of trappable iodine atoms is about $\sim 5 \times 10^{-5}$. The effective volume of the magnetic trap is estimated to be ~ 0.30 cm^3.

In fact, the high voltage for precursor orientation can be pulsed on when the ICl molecules come. After photostop, it can be switched off on a time order of ~ 1 μs, as demonstrated in the Stark deceleration,[21] to reduce interference in atom trapping.

4. Discussion and conclusions

In conclusion, we have theoretically studied the Photostop of iodine atoms from electrically oriented ICl molecules. The dynamical photofragmentation of the ICl precursors has been simulated using the Monte Carlo method based on their orientational probability distribution functions. The velocity distributions of the iodine atoms produced and their corresponding production rates have been analyzed for orienting electrical fields of various intensities. For ICl precursor beams with an initial rotational temperature of ~ 1 K, the production of the photostopped iodine atoms near zero speed can be improved by ~ 5 times with an orienting E-field intensity of ~ 200 kV/cm. For instance, the production rate for iodine atoms with speeds less than ~ 10 m/s is $\sim 0.5‰$. The photostopped iodine atoms near zero speed are good candidates for trapping experiments. By using a pair of charged ring magnets, the electrical orientation of ICl precursors and magnetic trapping of photostopped iodine atoms *in situ* can be conveniently realized. The electrical field generated by the HV charged ring magnets has been obtained numerically with strong electrical fields appearing in between for precursor orientation. The magnetic trap is able to confine I ($^2P_{3/2}$) atoms in the low field seeking $J_m = 1/2$ and 3/2 states with a maximal trapping speed of ~ 4.0 m/s and ~ 7.0 m/s, respectively. The ICl molecular beams from supersonic expansion readily have densities of about 10^{12}–10^{14} cm^{-3}. With a volume of about 0.01 cm^3 for the ICl precursor beams used for Photostop and a volume of ~ 0.30 cm^3 for the magnetic trap, the total number of magnetically trapped iodine atoms is about 5×10^5–10^7 with densities on the order of 10^6–10^8 cm^{-3}. The above values can be further increased if more strong orienting E-fields or lower rotational temperatures of the precursor beams are used. Scientific interest in studying iodine has been strong for a rather long time and photostopped or even trapped iodine atoms would serve as a good starting point for other researches.

References

[1] Anderson M H, Ensher J R, Matthews M R, Wieman C E and Cornell E A 1995 *Science* **269** 198
[2] Anglin J R and Ketterle W 2002 *Nature* **416** 211
[3] Jones K M, Tiesinga E, Lett P D and Julienne P S 2006 *Rev. Mod. Phys.* **78** 483
[4] Kohler T, Goral K and Julienne P S 2006 *Rev. Mod. Phys.* **78** 1311
[5] Maxwell S E, Barhms N, Decarvalho R, Glenn D R, Helton J S, Nguyen S V, Patterson D, Petricka J, Demille D and Doyle J M 2005 *Phys. Rev. Lett.* **95** 173201
[6] Rangwala S A, Junglen T, Rieger T, Pinkse P W H and Rempe G 2003 *Phys. Rev. A* **67** 043406
[7] Bethlem H L, Berden G and Meijer G 1999 *Phys. Rev. Lett.* **83** 1558
[8] Vanhaecke N, Meier U, Andrist M, Meier B and Merkt F 2007 *Phys. Rev. A* **75** 031402
[9] Fulton R, Bishop A I and Baker P F 2004 *Phys. Rev. Lett.* **93** 243004
[10] Doherty W G, Bell M T, Softley T P, Rowland A, Wrede E and Carty D 2011 *Phys. Chem. Chem. Phys.* **13** 8441
[11] Trottier A, Wrede E and Carty D 2011 *Mol. Phys.* **109** 725
[12] Zhao B S, Shin S E, Park S, Sun T X and Chung D S 2009 *J. Phys. Soc. Jpn.* **78** 094302
[13] Rennick C J, Lam J, Doherty W G and Softley T P 2014 *Phys. Rev. Lett.* **112** 023002
[14] Deng L Z and Yin J P 2014 *J. Chem. Phys.* **141** 164314
[15] Devries M S, Vanveen N J A, Hutchinson M and Devries A E 1980 *Chem. Phys.* **51** 159
[16] Bazalgette G, White R, Tre'Nec G, Audouard E, Buchner M and Vigue J 1998 *J. Phys. Chem. A* **102** 1098
[17] Friedrich B and Herschbach D R 1991 *Nature* **353** 412
[18] Wu M, Bemish R J and Miller R E 1994 *J. Chem. Phys.* **101** 9447
[19] Liao Y Y, Chen Y N and Chuu D S 2004 *Phys. Rev. B* **70** 233410
[20] Kumarappan V, Bisgaard C Z, Viftrup S S, Holmegaard L and Stapelfeldt H 2006 *J. Chem. Phys.* **125** 194309
[21] Bethlem H L, Berden G and Meijer G 1999 *Phys. Rev. Lett.* **83** 1558